Available online at www.sciencedirect.com
ScienceDirect
Catalysis Today 130 (2008) 117–125
CATALYSIS TODAY
www.elsevier.com/locate/cattod

On the interaction between Co- and Mo-complexes in impregnation solutions used for the preparation of Al_2O_3-supported HDS catalysts: A combined Raman/UV–vis–NIR spectroscopy study

Jaap A. Bergwerff, Tom Visser, Bert M. Weckhuysen *

Inorganic Chemistry and Catalysis Group, Department of Chemistry, Utrecht University, Sorbonnelaan 16, 3584 CA Utrecht, The Netherlands

Available online 9 August 2007

Abstract

Research has been carried out on the formation of cobalt (Co) and molybdenum (Mo) complexes in CoMo-solutions, which are used for the preparation of Al_2O_3-supported hydrodesulphurization (HDS) catalysts. Aim of this study was to obtain more insight into possible Co–Mo interactions and their implications for the impregnation process. For this purpose, Raman and UV–vis–NIR spectroscopy has been carried out on different impregnation solutions at various pH. In addition, multivariate curve resolution (MCR) of the Raman spectra has been applied to obtain information on the molecular structure and speciation of the different complexes present in solution. Furthermore, Raman microscopy and SEM-EDX were applied on Al_2O_3 extrudates after impregnation, to obtain information on the distribution of the different metal-ions into the catalyst body as a function of time. It is demonstrated that an interaction between Co(II)-cations and different molybdate anions is indeed present in CoMo-solutions. Two different CoMo-complexes are proposed in which Co^{2+}-cations are bound to the outside of $H_xMo_7O_{24}^{(6-x)-}$ complexes, resulting in a simultaneous transport of the Co and Mo metal–precursor complexes. Since Co acts as a promotor, a close interaction between Co and Mo in the final catalyst is of major importance for the catalytic activity. As such, the interaction should also be taken into account in the preparation of supported CoMo–HDS catalysts.

Keywords: CoMo/Al_2O_3; Catalyst preparation; Raman spectroscopy; UV–vis–NIR spectroscopy; Multivariate curve resolution; Micro-spectroscopy

1. Introduction

Understanding the interaction between a metal-ion precursor and a support surface is a prerequisite for a controlled preparation of supported catalysts [1–3]. Especially in the field of supported (Co/Ni)Mo hydrodesulphurization catalysts, this interaction has a large influence on the nature and dispersion of the (Co/Ni)MoS_2-phase and hence on the activity of the final catalyst. It is therefore of prime importance to know the speciation of metal-ion complexes in impregnation solutions. The classical precursor salt for the synthesis of Mo(VI)-containing impregnation solutions is $(NH_4)_6Mo_7O_{24}$ (AHM). For that reason, the speciation of Mo(VI)-complexes in AHM-solutions has been extensively studied and well established [4–8]. Potentiometric titrations and spectroscopic techniques have been applied to derive formation constants of the different anions that can be present in aqueous solution. It was found that tetrahedral MoO_4^{2-} anions are present at low Mo-concentrations and high pH. The formation of isopolyanions takes place at higher concentrations in acidic solutions, while $H_xMo_7O_{24}^{(6-x)-}$complexes are found to be dominant in solutions of pH 3–6. At lower pH the formation of larger clusters, such as $H_xMo_8O_{26}^{(4-x)-}$ has been reported as well. Furthermore, Mo-isopolyanions are known to react with various cations in solution to form so-called heteropolyanions. The complexation of trivalent cations, such as Al^{3+} [8,9], Cr^{3+} [10] and Co^{3+} [11] by Mo-anions has been demonstrated to result in the formation of Anderson-type complexes in acidic environment. Murase et al. reported on the formation of complexes with $NiMo_6$ stoichiometry in acidic NiMo solutions, for which they propose a similar structure [6]. In view of these findings, it is a logical step to study a possible interaction between Co^{2+}-cations and Mo-anions in CoMo-solutions in the absence of complexing agents.

* Corresponding author. Tel.: +31 30 253 4328; fax: +31 30 251 1027.
E-mail address: b.m.weckhuysen@chem.uu.nl (B.M. Weckhuysen).

0920-5861/$ – see front matter © 2007 Elsevier B.V. All rights reserved.
doi:10.1016/j.cattod.2007.06.037

This paper describes the results of a characterization study to determine the formation of Mo(VI)-complexes in AHM and AHM/$Co(NO_3)_2$ solutions as a function of pH, using UV–vis–NIR and Raman spectroscopy. The speciation of the different isopolymolybdate complexes and their reference spectra have been derived by means of multivariate curve resolution (MCR). In addition, SEM-EDX and Raman microscopy have been used to evaluate the effect of the interaction between Co^{2+}-cations and Mo-anions on the transport rate of these complexes inside Al_2O_3 extrudates after impregnation, since these spatially resolved techniques are known to be useful to elucidate the chemical and physical processes that play a role during the preparation of supported catalyst bodies [12–14].

2. Experimental

The compositions of the solutions used for spectroscopic studies are listed in Table 1. $(NH_4)_6Mo_7O_{24}$ (Acros, p.a.) and $Co(NO_3)_2{\cdot}6H_2O$ (Acros, p.a.) were used for the preparation of these solutions. For Raman measurements on Mo-solutions, NH_4NO_3 (Acros, p.a.) was added to serve as an internal standard. Concentrated NaOH (Merck, p.a.) and HCl (Merck, p.a.) solutions were used for pH adjustment. Care was taken that the concentration of the components under study was not altered during measurements.

Raman spectra were recorded on the different solutions using a Kaiser RXN spectrometer equipped with a 70 mW, 532 nm diode laser for excitation. The data point resolution in these spectra, which were subject to baseline correction before analysis, is 2 cm^{-1}. The NO_3^- peak at 1044 cm^{-1} was used as an internal standard and spectra were scaled to this band. UV–vis–NIR measurements (250–1100 nm) were carried out on the solutions in series 2 using a Varian Cary 50 spectrophotometer equipped with a Hellma immersion probe. UV–vis–NIR spectra were recorded on the solutions in series 3 in the spectral range of 200–1350 nm on a Varian Cary 500 spectrophotometer with water as the reference. The data point resolution of the UV–vis–NIR measurements was 1 nm. All measurements were carried out under ambient conditions (298 K).

Impregnation was carried out on cylindrical Al_2O_3 extrudates of 1.5 mm diameter and an average length of 10 mm. The pore volume of this material was 0.80 ml/g and its surface area was 300 m^2/g. Impregnation was carried out on 20 g batches of extrudates with a 1.0 M Mo/0.2 M Co solution prepared from AHM and $Co(NO_3)_2$. Care was taken that the extrudates were completely wetted by the solution. Drying was carried out by passing hot air onto the wet extrudates. Drying was regarded to be complete when the temperature of the catalyst bed had reached 120 °C. One batch of material was dried 5 min after impregnation, while another batch was allowed to age in a closed container for 3 h before drying. Scanning electron microscopy was performed in combination with energy-dispersive analysis of X-rays (EDX). Samples were embedded in Castoglas and polished on SiC paper with 2-propanol. Samples were then carbon-coated and line scans were recorded across the cross-section of bisected extrudates with a step-size of 10 μm at a 20 kV acceleration voltage. For comparison, extrudates were also impregnated with a 1.0 M Mo AHM-solution and a 0.2 M $Co(NO_3)_2$ solution. Raman spectra were recorded on bisected dried extrudates using a Kaiser RXN spectrometer equipped with a 785 nm diode laser in combination with a Hololab 500 Raman microscope. A 10× objective was used for beam focusing and collection of scattered radiation, resulting in a spot size on the sample of approximately 50 μm diameter. The extrudates were calcined at 500 °C for 1 h in static air. Upon calcination the color of the samples containing Co changes from pink to blue, which made it easier to observe the distribution of this metal-ion in bisected extrudates.

Table 1
Composition of Mo- and CoMo-solutions used for spectroscopic studies

[Mo] (*M*)	[Co] (*M*)	[NO_3^-] (*M*)	pH	*n*	Technique
0.1	–	0.1	2.11–8.24	26	Raman
0.1	0.1	0.1	2.00–5.96	19	Raman
					UV–vis–NIR
0–0.40	0.04	0.08	5.0	8	UV–vis–NIR

The concentration (*M*), the pH range, the technique applied and the number of spectra (*n*) that were recorded in each titration series are included.

3. Results and discussion

3.1. Mo-solutions

In industrial catalyst preparation, impregnation solutions with high Mo-concentrations (typically exceeding 1.0 M Mo) are used to obtain high Mo-loadings in the final catalyst. However, at these concentrations, formation of larger Mo(VI)-clusters at low pH results in the precipitation of Mo(VI)-salts. Hence, for the spectroscopic investigations described in this section, 0.10 M Mo AHM-solutions were used to study the speciation of Mo(VI)-complexes in a broad pH range. The reaction equations for the formation of $H_xMo_7O_{24}^{(6-x)-}$ and $H_xMo_8O_{26}^{(4-x)-}$ polyanions from MoO_4^{2-} under acidic conditions are given in Eqs. (1) and (2). The formation constants of the complexes as formulated in Eq. (3), have been determined by different authors with the aid of potentiometric titrations [6–8]. In some cases, the formation of polyanions consisting of 2 or 19 Mo-atoms was proposed, as well. The molecular formulas of the isopolyanions that were considered in the models proposed in the different publications are listed in Table 2 [7].

$$7MoO_4^{2-} + (8+x)H^+ \leftrightarrow H_xMo_7O_{24}^{(6-x)-} + 4H_2O \quad (1)$$

$$8MoO_4^{2-} + (12+x)H^+ \leftrightarrow H_xMo_8O_{26}^{(4-x)-} + 6H_2O \quad (2)$$

$$\beta_{mp} = \frac{[H_xMo_mO_y]}{[MoO_4^{2-}]^m[H^+]^p} \quad (3)$$

Raman spectra recorded on 0.10 M Mo solutions in the pH range 2–8 are presented in Fig. 1. The theoretical speciation of Mo(VI)-complexes in these solutions was determined from the formation constants of isopolyanions reported by different authors [4,7,8,15]. The resulting concentration plots are

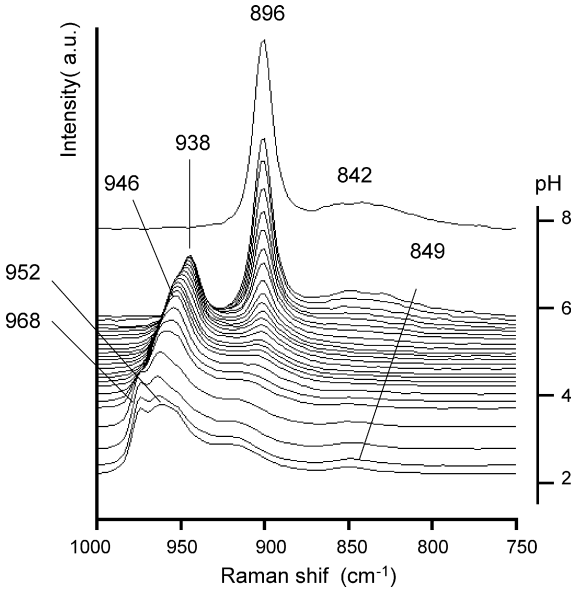

Fig. 1. Selected Raman spectra recorded on the 0.10 M Mo AHM-solutions in series 1 at different pH values in the pH range 2–8.

presented in Fig. 2a–c. As can be seen from Fig. 1, the spectra recorded on AHM-solutions of pH 6 (or higher) show bands at 896 cm^{-1} and 842 cm^{-1} due to symmetric and anti-symmetric Mo=O stretching vibrations and a band at 318 cm^{-1} (not shown) as a result of a O=Mo=O bending vibration. These features are characteristic of MoO_4^{2-} in solution, in accordance with the speciation plot. When the pH is decreased, $Mo_7O_{24}^{6-}$ starts to be formed and a band appears at 938 cm^{-1}. A further decrease in pH to a value of 4.5 leads to a shift in the most intense Mo=O stretching band to higher wavenumber. Probably, this shift is the result of the protonation of $Mo_7O_{24}^{6-}$, which is observed in the same pH region in Fig. 2a–c. At a pH lower than 3, multiple Mo=O stretching vibration bands are observed (968 cm^{-1} and 952 cm^{-1}) along with a new feature at 849 cm^{-1}. In the speciation plot, the formation of $H_3Mo_7O_{24}^{3-}$, $Mo_8O_{26}^{4-}$ and $HMo_8O_{26}^{3-}$ is observed at these pH values.

Since the solutions under study contain a number of different Mo(VI)-complexes, the measured spectra are the result of contributions from these different components. With the aid of a chemometric procedure, called multivariate curve resolution (MCR), the Raman spectra can be deconvoluted into pure component spectra and the factors that describe their quantitative contributions to the measured spectra (the so-called scores). In general, this is achieved by solving the following equation.

$$X(n_{\text{spectra}} \times n_{\text{data points}}) = C(n_{\text{spectra}} \times n_{\text{comp.}})S(n_{\text{comp.}} \times n_{\text{data points}}) + E(n_{\text{spectra}} \times n_{\text{data points}}) \quad (4)$$

In this equation, X represents the data matrix, in this case containing the 26 Raman spectra (n_{spectra}) recorded on the AHM-solutions in series 1. For the chemometric analysis, spectra have been used in the range of 750–1000 cm^{-1} with 2 cm^{-1} data point resolution, yielding 126 data points ($n_{\text{data points}}$) for each spectrum. In general, the 250–450 cm^{-1} spectral range in which the O=Mo=O bending vibrations are observed, also contains valuable information on the nature of Mo(VI)-complexes in aqueous solution [16]. However, the intensity of these bands is much lower and the signal-to-noise ratio in this part of the spectrum was insufficient for a reliable quantitative analysis.

The matrix C contains the scores of a number of pure components ($n_{\text{comp.}}$) for all solutions on which spectra were recorded. The spectrum matrix S contains the pure component spectra. E is the residual error matrix, which consists of the difference between the measured spectra and the spectra constructed from a linear combination of the pure component spectra. Through an iteration procedure, in which the values in matrices C and S are systematically varied, the value of matrix E is minimized. In the MCR-procedure, the values in matrices C and S are forced to be positive, a prerequisite to obtain meaningful spectra. Furthermore, spectra thought to originate from the presence of one type of Mo(VI)-complex in solution

Table 2
Stoichiometry [m, p], molecular formula, formation constants (β_{mp}) [5] and positions of main Mo=O stretching bands of Mo(VI) isopolyanions in solution

Complex [m, p]	Formula	Log(β_{mp})				Component	Raman bands (cm^{-1})
		[7]	[8]	[15]	[4]		
$[1,0]^{2-}$	MoO_4^{2-}	–	–	–		Mo-1	896, 842
$[1,1]^{-}$	$HMoO_4^{-}$	3.55	3.39	4.00			
[1,2]	H_2MoO_4	7.22	7.35	7.50			
$[7,8]^{6-}$	$Mo_7O_{24}^{6-}$	52.81	52.42	57.70	53.18	Mo-2	939, 896
$[7,9]^{5-}$	$HMo_7O_{24}^{5-}$	57.40	57.23	62.14	56	Mo-3	946, 904
$[7,10]^{4-}$	$H_2Mo_7O_{24}^{4-}$	60.97	60.78	65.60		Mo-4	958, 912
$[7,11]^{3-}$	$H_3Mo_7O_{24}^{3-}$	63.03		68.34		Mo-5	–
$[8,12]^{4-}$	$Mo_8O_{26}^{4-}$	71.19	71.62		69.73	Mo-5	–
$[8,13]^{3-}$	$HMo_8O_{26}^{3-}$	73.03	73.38			Mo-5	–
$[8,15]^{-}$	$H_3Mo_8O_{26}^{-}$		76.34				
[19,34]				196.3			
[2,5]				19.0			

The stoichiometry of the complexes is defined as the number of MoO_4^{2-} (m) and H^+ (p) required for their formation, as described in Eqs. (1)–(3).

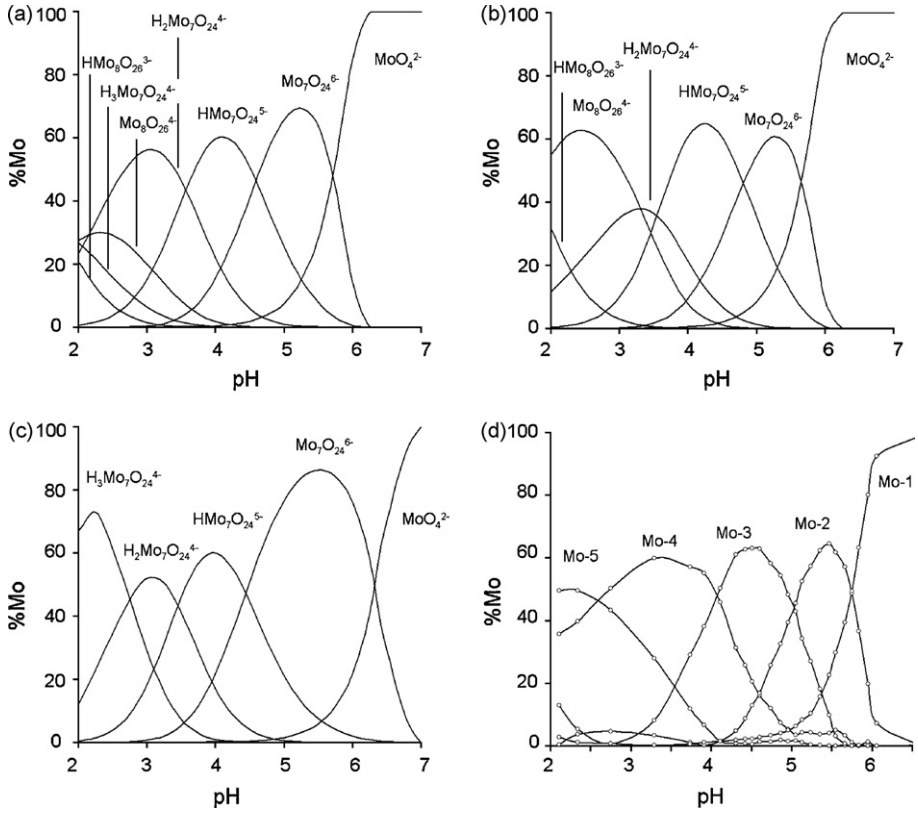

Fig. 2. Theoretical speciation plot of Mo(VI)-complexes in 0.10 M Mo (AHM) solutions as a function of pH derived from formation constants reported by (a) Tytko et al. [7], (b) Petterson et al. [15], (c) Ohman [8] and (d) the speciation plot of components Mo-1 to Mo- 5 in 0.10 M Mo (AHM) solutions derived from MCR analysis of Raman spectra.

can be used as input in matrix *S*, prior to the iteration procedure. In this way, the measured spectra are deconvoluted into the spectra and the scores of the different components that are simultaneously present in solution. The algorithms used for the MCR analysis can be found in references [17,18]. When it is assumed that all Mo(VI)-complexes in solution are Raman active, the concentrations of the different Mo(VI)-complexes can be calculated from the scores of the different components.

Using MCR, the best fit of the spectra recorded on the 0.10 M Mo AHM-solutions was obtained with five components, Mo-1 to Mo-5. After the iteration procedure, the absolute values in the error matrix were on average 1.6% of the values in the corresponding data matrix. The result is shown in Fig. 2d, where the lines indicate the concentration of the five different components as a function of the pH. By comparison to the speciation plots in Fig. 2a–c, it can be concluded that the scores of components Mo-1, Mo-2 and Mo-3 represent the concentration of MoO_4^{2-}, $Mo_7O_{24}^{6-}$ and $HMo_7O_{24}^{5-}$ anions, respectively. In the pH range, where the concentration of components Mo-4 is at a maximum, $H_2Mo_7O_{24}^{4-}$ is the predominant component in the theoretical speciation plots. The presence of component Mo-5 at pH 2–3 indicates that this species represents the formation of $H_3Mo_7O_{24}^{3-}$, $Mo_8O_{26}^{4-}$ and $HMo_8O_{26}^{3-}$ complexes. Although these complexes are expected to give rise to different Raman spectra, a more detailed deconvolution of the contributions of these different complexes was not possible. The deconvoluted Raman spectra of components Mo-1 to Mo-5 are presented as the solid lines in Fig. 3. The assignment of the different components to actual Mo(VI)-complexes and the Raman band maxima are included in Table 2. The positions of the Mo=O stretching vibration bands are in good agreement with values reported for different Mo(VI) isopolyanions in the literature [16,19].

3.2. CoMo-solutions

The interaction between Co(II) and Mo(VI)-anions was evaluated by Raman and UV–vis–NIR spectroscopic analysis of the CoMo-solutions. UV–vis–NIR spectra recorded on 0.04 M Co(II) solutions with varying Mo-concentrations (0–0.4 M) are presented in Fig. 4. In these solutions, the pH was kept constant at a value of 5.0. The spectrum of the solution without Mo, shows absorption bands at 511 nm (with a shoulder at 475 nm) and 1256 nm, corresponding to d–d transitions of the $[Co(H_2O)_6]^{2+}$ complex [20]. The part of the spectrum at shorter wavelengths could not be used due to the strong adsorption of water in this spectral range. Addition of AHM and the introduction of Mo(VI)-anions lead to a considerable increase in intensity and a slight red shift in the maxima of both bands. At a Mo:Co ratio of 10, the band maxima are located at 515 nm and 1262 nm and the intensity of the bands has increased by a factor 2.3 (515 nm) and 1.5 (1262 nm). The spectrum of a 0.40 M Mo AHM-solution of pH 5.0 without Co(II) is included in the same figure. It can be observed that the

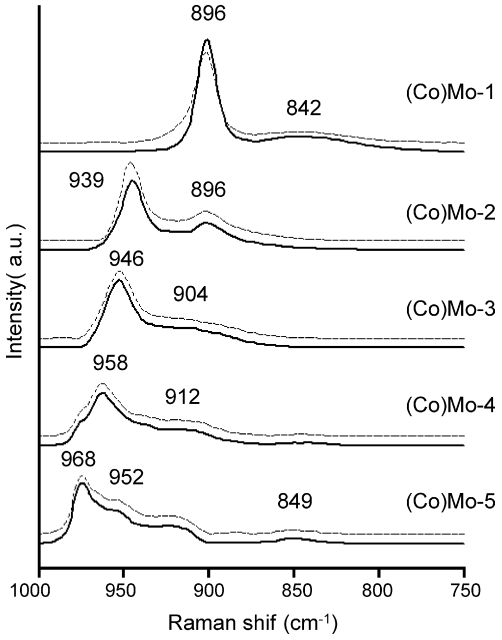

Fig. 3. Solid lines: pure spectra of components Mo-1 to Mo-5 (top to bottom) obtained from MCR analysis of the Raman spectra recorded on 0.10 M Mo solutions. Dashed lines: components CoMo-1 to CoMo-5 obtained from MCR analysis of the Raman spectra recorded on 0.10 M Mo/0.10 M Co solutions.

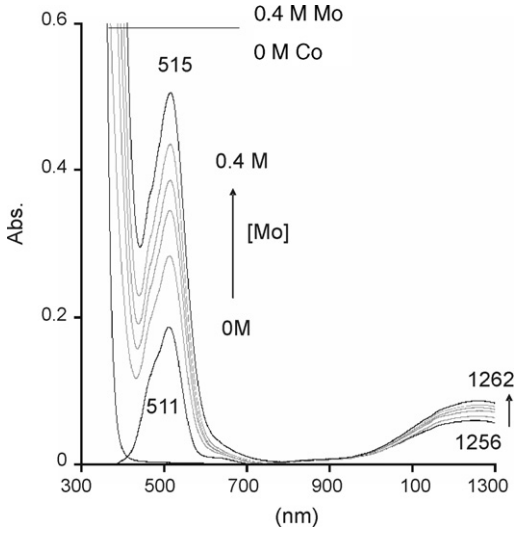

Fig. 4. Selected UV–vis–NIR spectra recorded on the 0.04 M Co solutions with different Mo-concentrations (0–0.40 M) in series 3. The pH of all solutions was 5. The spectrum of a 0.40 M Mo solution of the same pH is included for comparison.

presence of Co(II) results in a red shift in the Mo(VI)–O charge transfer band. From the changes in the UV–vis–NIR spectra, it can be inferred that a chemical interaction must exist between Co(II)- and Mo(VI)-complexes in these solutions at pH 5.0.

In analogy to the experiment described above, UV–vis–NIR and Raman spectroscopy were applied to 0.10 M Mo AHM-solutions of different pH in the presence of 0.10 M $Co(NO_3)_2$ (series 2). The resulting Raman spectra are presented in Fig. 5a and the UV–vis–NIR data in Fig. 5b. In the latter spectra, a continuous increase in the d–d transition band of Co(II) is observed upon increasing the pH of the CoMo-solutions. At the same time, the onset of the Mo(VI)–O charge transfer band shifts to higher wavelength (pH 2–5) and back (pH 5–6). The position of the onset of this band is reported to be a function of the number of Mo-atoms in a Mo(VI)-isopolyanion [21], although an interaction with Co(II)-complexes may also influence the position of these bands. Due to the high intensity of the Mo(VI)–O charge transfer bands interpretation is rather complicated since the position of the maxima cannot be determined. By comparison of Fig. 5a to Fig. 1, it can be seen that at pH ≈ 2, the Raman spectra recorded on Mo- and on CoMo-solutions are remarkably similar. At a pH between 3 and 4.5 a shift in the most intense Mo=O stretching vibration to a final value of 941 cm^{-1} is observed. However, compared to the spectra recorded on the Mo-solutions, this shift takes place at lower pH, which confirms an interaction with Co. From pH 5, the formation of MoO_4^{2-} is again observed by the appearance of a band at 896 cm^{-1}. Finally, at pH ≈ 6 the formation of a purple precipitate ($CoMoO_4$) was observed.

Next, MCR-analysis of the Raman spectra was carried out, using the same parameters as for the deconvolution of Raman

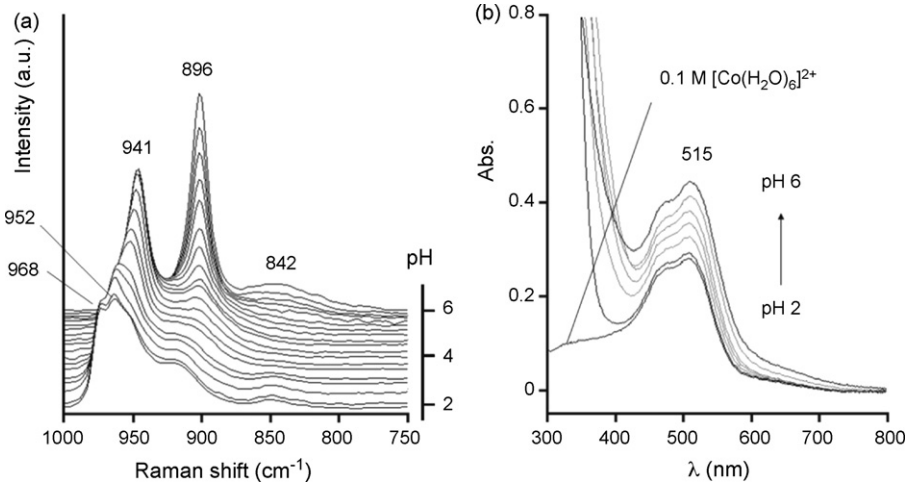

Fig. 5. Selected Raman (a) and UV–vis–NIR (b) spectra recorded on the 0.10 M Mo/0.10 M Co solutions in series 2 at different pH values in the pH range 2–6.

spectra recorded on the cobalt-free Mo-solutions. This time, the goodness of fit, defined as the overlap between the measured spectra and the fitted spectra was 98.3%. The thus obtained spectra of components CoMo-1 to CoMo-5 are presented as the dotted lines in Fig. 3. As appears, the spectra are practically identical to the spectra Mo-1 to Mo-5 obtained from the MCR-analysis of the Mo-solutions. It follows that the presence of Co(II) does not affect the structure of Mo(VI)-complexes in aqueous solution to a large extent.

In contrast, the concentration profiles of components CoMo-1 to CoMo-5 in the CoMo-solutions, as calculated from the MCR-analysis, clearly point to an effect of Co on the formation of the Mo-complexes. This is illustrated in Fig. 6, where the speciation plots of components CoMo-1 to CoMo-5 (solid lines) have been plotted together with the concentration profiles of Mo-1 to Mo-5 (dotted lines). It is evident that the maxima in the concentration profiles of the different $H_xMo_7O_{24}^{(6-x)-}$ complexes have shifted to lower pH after the addition of $Co(NO_3)_2$. Apparently, the presence of Co(II) induces deprotonation of these Mo-complexes. The intensity of the d–d transition band of Co(II), which is presented in the same figure as a grey line, was determined at 550 nm, to avoid any influence of the Mo(VI)–O charge transfer band. The slope of this line indicates, that a correlation exists between the formation of deprotonated heptamolybdates (components Mo-2 and Mo-3) and the increase of the Co(II) d–d transition band in the UV–vis–NIR spectra. In our opinion, coordination of Co(II) to the outside of the $HMo_7O_{24}^{5-}$ and $Mo_7O_{24}^{6-}$ anions is a plausible explanation for both observations. Apparently, Co(II) is preferentially coordinated by more and more deprotonated (and thus more negatively charged) $H_xMo_7O_{24}^{(6-x)-}$ anions. Inversely, this results in the deprotonation of heptamolybdate anions at lower pH when Co(II) is present. It follows, that complexation leads to the exchange of one or two water ligands of the $[Co(H_2O)_6]^{2+}$ complexes by one or two terminal oxygen atoms from the Mo(VI)-anions. This explains the increased intensity of the d–d transition bands, since the coordination sphere of Co(II) is no longer perfectly octahedral. However,

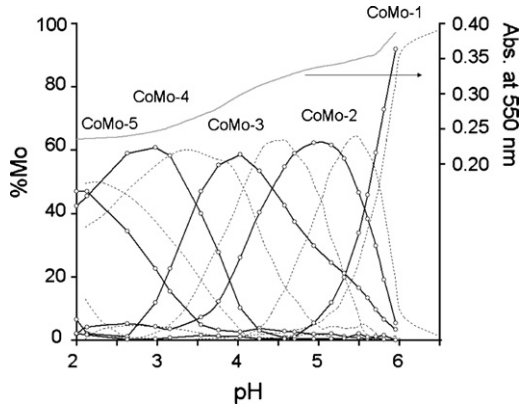

Fig. 6. Speciation plots of components CoMo-1 to CoMo-5 obtained from MCR analysis of Raman spectra recorded on 0.10 M Mo/0.10 M Co solutions (solid lines) and components Mo-1 to Mo-5 derived from 0.10 M Mo solutions (dashed lines). The absorbance at 550 nm in the UV–vis–NIR spectra recorded on 0.10 M Mo/0.10 M Co solutions is indicated by the gray line.

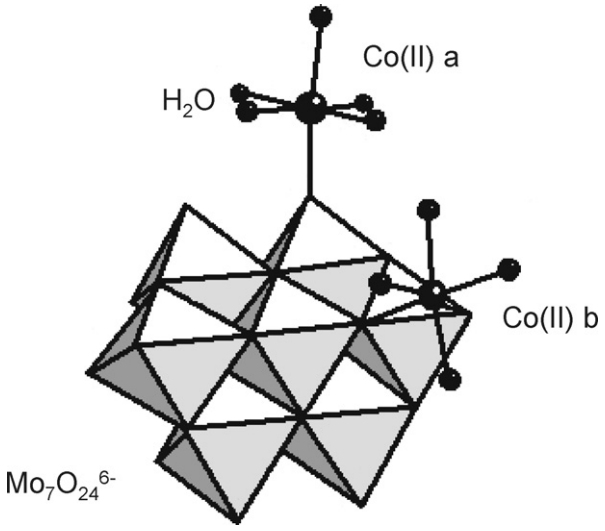

Fig. 7. Tentative structure of $Co_2Mo_7O_{24}^{2-}$ complexes present in CoMo-solutions based on the crystal structure of $[(Fe)_2(H_2O)_9Mo_7O_{24}]^{2-}$ and $[(Mn)_2(H_2O)_9Mo_7O_{24}]^{2-}$ complexes reported by Long et al. [21].

regarding the small shift of the d–d bands, Co(II) must be still almost octahedrally surrounded by oxygen atoms.

These conclusions are in good agreement with the results on the crystal structures of $[(Fe)_2(H_2O)_9Mo_7O_{24}]^{2-}$ and $[(Mn)_2(H_2O)_9Mo_7O_{24}]^{2-}$ cluster compounds, recently reported by Long et al. [22]. It was demonstrated that the complexation of the divalent cations takes place on the outside of the heptamolybdate anions. It seems reasonable to assume that $Co_2Mo_7O_{24}$ complexes could be formed in the CoMo-solutions with a similar configuration. The tentative molecular structure of these complexes, based on the structure of the Fe- and Mn-heptamolybdates, is presented in Fig. 7. In this figure, the coordination of the Co(II)-atoms to the $Mo_7O_{24}^{6-}$ complex via one oxygen (Co(II-a) or two oxygens (Co(II-b) is illustrated.

Finally, it should be noted that the intensity of the Co(II) d–d band increases even though disintegration of $Mo_7O_{24}^{6-}$ occurs at a pH > 5. Apparently, MoO_4^{2-} is able to coordinate to Co(II) in a similar manner as heptamolybdate complexes, without the formation of a $CoMoO_4$ precipitate. The proposed complexation of Co(II) by Mo(VI)-anions seems to provide a plausible explanation for the observed spectroscopic features.

3.3. Impregnation of Al_2O_3 extrudates with CoMo-solutions

Fig. 8 shows four images of bisected calcined extrudates prepared from three different solutions, i.e., 1.0 M Mo AHM/0.2 M $Co(NO_3)_2$, 0.2 M $Co(NO_3)_2$ and 1.0 M Mo AHM. The 1.0 M Mo AHM/0.2 M $Co(NO_3)_2$-impregnated extrudates that were dried without ageing (5 min) showed an egg-shell distribution of the Co^{2+}-complexes. This was confirmed by calcination, since the blue color of Co^{2+}, tetrahedrally coordinated by oxygen ligands, was only observed near the external surface of the extrudates. Likewise, Raman line scanning of these extrudates revealed the presence of Mo^{6+} complexes only in the outer ring of the extrudates, since the

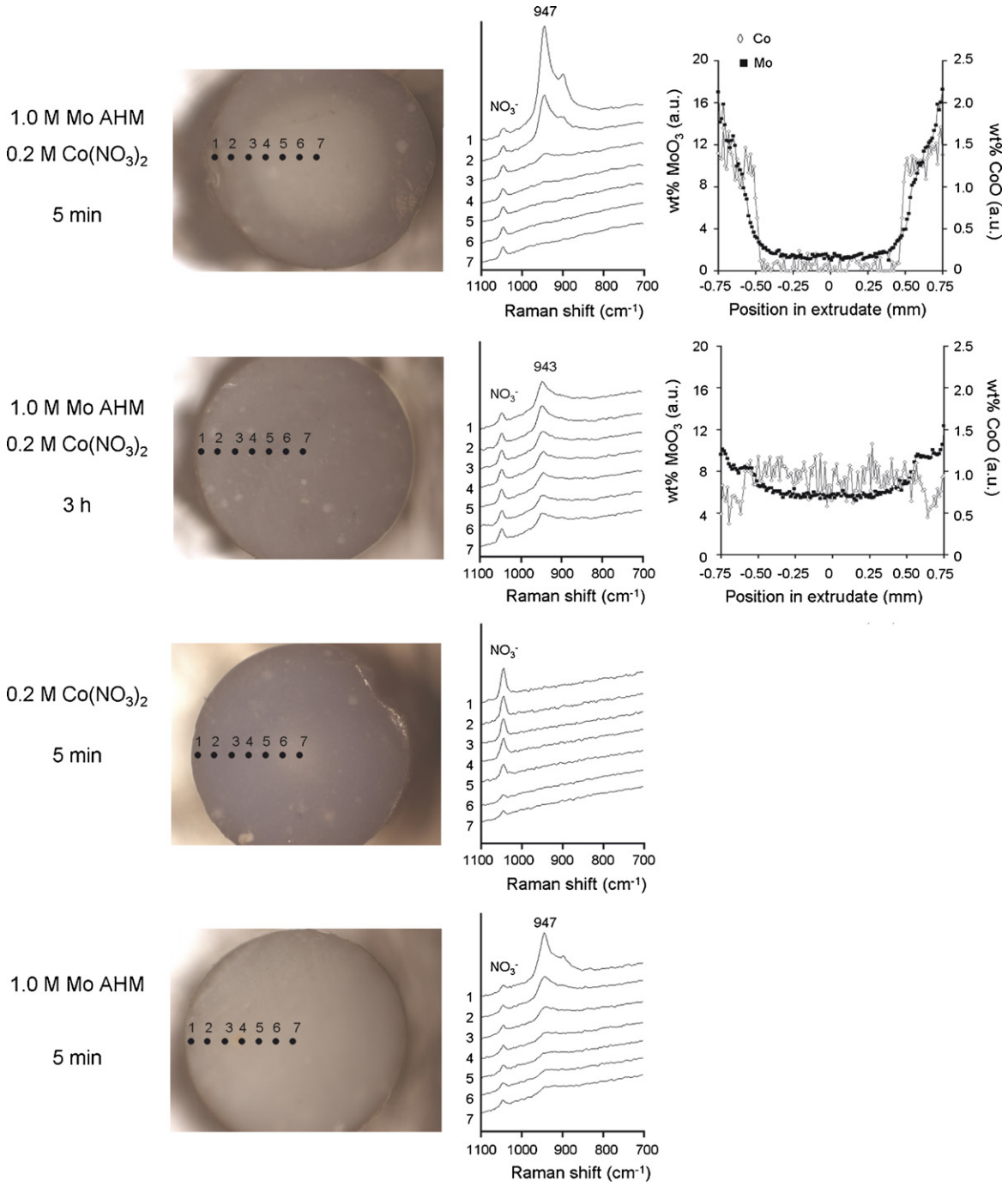

Fig. 8. Microscope images of calcined extrudates (left), Raman spectra recorded at different positions inside dried extrudates (middle) and Co and Mo-profiles obtained from SEM-EDX measurements (right) of samples prepared from different solutions, as indicated on the left.

corresponding ν(Mo=O) bands were merely observed at these positions. Furthermore, the formation of a white precipitate was established at the external surface of the extrudates. This precipitate was identified as $Al(OH)_6MoO_{18}^{3-}$ based on the characteristic Raman bands of this complex at 947 cm^{-1}, 899 cm^{-1} and 590 cm^{-1} (not shown). NO_3^- was found to be present throughout the pellets, judging from the band at 1044 cm^{-1} in the Raman spectra. The metal–distribution plots obtained from EDX-line scans confirm these observations. An egg-shell distribution of both Co and Mo was found, although Co-complexes seem to have penetrated slightly further towards the center of the extrudates.

The same analyses were carried out on the extrudates that were allowed to age for 3 h before drying. These samples showed a blue color throughout the extrudate, indicating a homogeneous distribution of Co. The same holds for Mo, since ν(Mo=O) Raman bands were observed for all positions in the sample. From these Raman bands, the one at 943 cm^{-1} revealed the presence of $HMo_7O_{24}^{(6-x)-}$ complexes throughout the extrudates. The Co- and Mo-profiles obtained form SEM-EDX

measurements show a rather homogeneous distribution of both, although a slight enrichment of Mo was found near the external surface, whereas the Co-concentration was slightly lower at these positions.

In the extrudates prepared from the 0.2 M $Co(NO_3)_2$ solution, Co was found to be well-distributed, except for a small spot near the core of the extrudates, where no color is observed. For obvious reasons, the Raman spectra showed only peaks due to the presence of NO_3^-, but the intensity of the bands was considerably lower near the core of the extrudates. The catalyst bodies prepared from the 1.0 M Mo AHM-solution exhibited an egg-shell distribution of Mo, when ageing was omitted. Strong ν(Mo=O) bands were only observed near the external surface of the extrudates after drying.

3.4. The role of interactions in the impregnation process

Considering the impregnation of Al_2O_3 extrudates with an aqueous Co/Mo solution, it is obvious that this process starts with an instantaneous uptake of the solution. Consequently, the metal-complexes will be transported with the flow of the solution into the outer pores. However, adsorption of metal-ion complexes on the support surface may hamper further transport of the metal-ion precursor. If so, this will result in an egg-shell distribution of the metal-ion complexes, which can only be overcome by a time-consuming process of desorption and diffusion. Adversely, such differences in the distribution of metal complexes inside a catalyst body can also be used to obtain information on their interaction with the support surface. Recently, for instance, we were able to demonstrate from UV–vis–NIR and MRI measurements, that the affinity of $[Co(H_2O)_6]^{2+}$ complexes for an Al_2O_3 surface is rather limited [23,24]. It was shown that a homogeneous distribution of Co-complexes was obtained relatively short after impregnation with a 0.2 M $Co(NO_3)_2$ solution. In Fig. 8, it was shown that, when drying was carried out 5 min after impregnation, only the core of the extrudates did not yet contain Co. From the Raman micro-spectroscopy measurements presented in the same figure, it can be derived that NO_3^- anions are distributed inside the catalyst bodies in a similar fashion. Hence, since NO_3^- is the only counter ion in solution, the distribution of Co^{2+} can be inferred from the NO_3^- distribution.

The inhomogeneous distribution of Mo inside the catalyst bodies after impregnation with a 1.0 M Mo solution is in line with the conclusion from our previous Raman micro-spectroscopic study on the impregnation of Al_2O_3 bodies with AHM-solutions [12]. The inhomogeneity is largely attributed to the adsorption of the Mo complexes in acidic environment onto the Al_2O_3 surface and the formation of an $Al(OH)_6MoO_{18}^{3-}$ phase. Finally, it can be concluded that the transport of both Co and Mo metal-ion complexes in the 1.0 M Mo/0.2 M Co impregnation solution is rather slow, since an egg-shell distribution of these species is found in the extrudates that were dried 5 min after impregnation. In fact, the distribution profiles of both metals are rather similar. Apparently, the presence of $Mo_7O_{24}^{6-}$ anions results in a slower transport of Co^{2+} through the extrudates. NO_3^- anions, on the other hand, were found to be present throughout the sample, which implies that Co^{2+} and $H_xMo_7O_{24}^{(6-x)-}$ travel together. In our opinion, this gives further evidence for an interaction between the Co^{2+} metal-ion and the $H_xMo_7O_{24}^{(6-x)-}$ complexes in the impregnation solution. Nevertheless, the Co- and Mo-profiles obtained from EDX-line scans are not completely identical. This may be tentatively ascribed to the disintegration of the CoMo-complexes upon adsorption onto the Al_2O_3 surface. During penetration of the metal-complexes into the catalyst body, the formation of inner-sphere Mo(VI)-surface complexes might lead to the release of $[Co(H_2O)_6]^{2+}$ which has a limited interaction with the support. This would explain the presence of Co-complexes at positions closer to the center of the extrudates in the sample dried after 5 min of ageing. The strong interaction between Mo(VI)-complexes and the Al_2O_3 could account for the higher concentration of Mo near the edges of the extrudates in the samples aged for 3 h.

4. Concluding remarks

It is concluded that an interaction between Co(II)-cations and different molybdate anions exist in CoMo-solutions of various pH. Most probably, CoMo-complexes are formed in which Co(II) is bound to the outside of molybdate-ions, but further studies are required to elucidate the exact molecular structure. The observed interaction can have consequences for the preparation of supported CoMo–HDS catalysts. After impregnation of Al_2O_3 extrudates with an AHM/$Co(NO_3)_2$ solution, the interaction between Co^{2+}-cations and $H_xMo_7O_{24}^{(6-x)-}$ complexes will lead to a simultaneous transport of the Co and Mo metal–precursor complexes and since Co acts as a promotor in these catalysts, a close interaction between Co and Mo in the final catalyst is of prime importance for the catalytic activity.

In practice, impregnation solutions, consisting of heteropolyanions that contain both Co and Mo (such as $Co_2Mo_{10}O_{38}H_4^{6-}$) have been used as an approach to maximize the promoting effect of Co. Indeed, this resulted in catalyst materials with a much higher activity [11,25,26]. For the same reason, NH_4^+ free solutions were used for impregnation, forcing the Co^{2+} to act as a counter ion for Mo-anions [27,28]. From this point of view, the observed interaction of Co(II)- and Mo(VI)-complexes in simple AHM/$Co(NO_3)_2$ solutions is a remarkable finding. The fact that the preparation of catalysts from AHM/$Co(NO_3)_2$ solutions generally yields inefficient catalysts can than be explained in two ways: (1) by assuming the interaction between the $H_xMo_7O_{24}^{(6-x)-}$ anions and Co^{2+} is too weak to be retained after deposition of the metal-ion complexes onto the support surface, or (2) the presence of NH_4^+ allows for the formation of $(NH_4)_3[Al(OH)_6MoO_{18}]$ deposits and hence a decrease in the dispersion of the Mo-phase.

As a spin-off, the results of this study demonstrate that spectroscopic techniques, such as Raman, UV–vis–NIR and SEM-EDX, can provide valuable information on the interactions of metal-ion complexes in impregnation solutions by determination of the individual transport rates inside catalyst bodies. Besides, advanced curve resolution techniques allow

more detailed analysis of the structure and speciation of the different complexes present in solution.

Acknowledgments

The preparation of the $CoMo/Al_2O_3$ extrudates and the SEM-EDX analyses were carried out at the laboratories of Albemarle Catalysts BV in Amsterdam. Marcel Jansen is kindly acknowledged for valuable discussions and his assistance with the experiments.

References

[1] M. Che, O. Clause, C. Marcilly, in: G. Ertl, H. Knözinger, J. Weitkamp (Eds.), Preparation of Solid Catalysts, Wiley–VCH, Weinheim, 1999, p. 315.
[2] X. Hao, L. Quach, J. Korah, W.A. Spieker, J.R. Regalbuto, J. Mol. Catal. A: Chem. 219 (2004) 97.
[3] K. Bourikas, C. Kordulis, A. Lycourghiotis, Catal. Rev. Sci. Eng. 48 (2006) 363.
[4] T. Ozeki, H. Kihara, S. Hikime, Anal. Chem. 59 (1987) 945.
[5] J.J. Cruywagen, E.A. Rohwer, G.F.S. Wessels, Polyhedron 14 (1995) 3481.
[6] K. Murase, H. Ando, E. Matsubara, T. Hirato, Y. Awakura, J. Electrochem. Soc. 147 (2000) 2210.
[7] K.H. Tytko, G. Beathe, J.J. Cruywagen, Inorg. Chem. 24 (1985) 3132.
[8] L.O. Ohman, Inorg. Chem. 28 (1989) 3629.
[9] H.Y. Lee, K.M. Park, U. Lee, H. Ichida, Acta Cryst. C: Cryst. Struct. Commun. 47 (1991) 1959.
[10] H.Y. An, Y.G. Li, D.R. Xiao, E.B. Wang, C.Y. Sun, Cryst. Growth Des. 6 (2006) 1107.
[11] C.I. Cabello, I.L. Botto, H.J. Thomas, Appl. Catal. A: Gen. 197 (2000) 79.
[12] J.A. Bergwerff, T. Visser, B.R.G. Leliveld, B.D. Rossenaar, K.P. de Jong, B.M. Weckhuysen, J. Am. Chem. Soc. 126 (2004) 14548.
[13] L.G.A. van de Water, J.A. Bergwerff, T.A. Nijhuis, K.P. de Jong, B.M. Weckhuysen, J. Am. Chem. Soc. 127 (2005) 5024.
[14] A.A. Lysova, I.V. Koptyug, R.Z. Sagdeev, V.N. Parmon, J.A. Bergwerff, B.M. Weckhuysen, J. Am. Chem. Soc. 127 (2005) 11916.
[15] L. Pettersson, I. Andersson, L.-O. Öhman, Inorg. Chem. 25 (1986) 4726.
[16] G. Mestl, T.K.K. Srinivasan, Catal. Rev. Sci. Eng. 40 (1998) 451.
[17] W. Windig, J. Guilment, Anal. Chem. 63 (1991) 1425.
[18] K. Schostack, P. Parekh, S. Patel, E.R. Malinowski, J. Res. Nat. Bur. Stand. 93 (1988) 256.
[19] R. Iwamoto, J. Grimblot, J. Adv. Catal. 44 (2000) 417.
[20] A.B.P. Lever, Inorganic Electronic Spectroscopy, Elsevier, Amsterdam, 1984.
[21] R.S. Weber, J. Catal. 151 (1995) 470.
[22] D.L. Long, P. Kogerler, L.J. Farrugia, L. Cronin, Dalton Trans. (2005) 1372.
[23] J.A. Bergwerff, A.A. Lysova, L. Espinosa Alonso, I.V. Koptyug, B.M. Weckhuysen, Angew. Chem. Int. Ed. 46 (2007) 7224.
[24] J.A. Bergwerff, L.G.A. van de Water, T. Visser, P. de Peinder, B.R.G. Leliveld, K.P. de Jong, B.M. Weckhuysen, Chem. Eur. J. 11 (2005) 4592.
[25] A. Griboval, P. Blanchard, L. Gengembre, E. Payen, M. Fournier, J.L. Dubois, J.R. Bernard, J. Catal. 188 (1999) 102.
[26] C. Martin, C. Lamonier, M. Fournier, O. Mentre, V. Harle, D. Guillaume, E. Payen, Chem. Mater. 17 (2005) 4438.
[27] D. Nicosia, R. Prins, J. Catal. 234 (2005) 414.
[28] D. Nicosia, R. Prins, J. Catal. 229 (2005) 424.